Stabilizing the Closed S6 Gate in the Shaker K_v Channel Through Modification of a Hydrophobic Seal

Tetsuya Kitaguchi, Manana Sukhareva, and Kenton J. Swartz

Molecular Physiology and Biophysics Section, National Institute of Neurological Disorders and Stroke, National Institutes of Health, Bethesda, MD 20892

ABSTRACT The primary activation gate in K^+ channels is thought to reside near the intracellular entrance to the ion conduction pore. In a previous study of the S6 activation gate in Shaker (Hackos et al., 2002), we found that mutation of V478 to W results in a channel that cannot conduct ions even though the voltage sensors are competent to translocate gating charge in response to membrane depolarization. In the present study we explore the mechanism underlying the nonconducting phenotype in V478W and compare it to that of W434F, a mutation located in an extracellular region of the pore that is nonconducting because the channel is predominantly found in an inactivated state. We began by examining whether the intracellular gate moves using probes that interact with the intracellular pore and by studying the inactivation properties of heterodimeric channels that are competent to conduct ions. The results of these experiments support distinct mechanisms underlying nonconduction in W434F and V478W, suggesting that the gate in V478W either remains closed, or that the mutation has created a large barrier to ion permeation in the open state. Single channel recordings for heterodimeric and double mutant constructs in which ion conduction is rescued suggest that the V478W mutation does not dramatically alter unitary conductance. Taken together, our results suggest that the V478W mutation causes a profound shift of the closed to open equilibrium toward the closed state. This mechanism is discussed in the context of the structure of this critical region in K^+ channels.

KEY WORDS: voltage-dependent gating • closed gate • Agitoxin • mutagenesis • potassium channel

INTRODUCTION

For most ion channel proteins, the ion conduction pathway is not always open, but is dynamically regulated so that the pore opens and closes in response to a particular stimulus (Hille, 2001). In voltage-gated potassium (K_v) channels, a K^+ selective pore opens and closes in response to changes in membrane voltage (Yellen, 1998). These channels are tetramers, with each subunit containing six transmembrane (TM) segments, designated S1 through S6 (Fig. 1 B). Some of the earliest functional studies on the gating of K_v channels in the squid giant axon suggest that the activation gate is located near the intracellular entrance to the ion conduction pore (Fig. 1 A) (Armstrong, 1969, 1971; Armstrong and Hille, 1972). More recent studies on the Shaker K_v channel support the notion of an intracellular activation gate, pointing to a specific region within the S6 TM where the access of methanesulfonates and silver ions changes quite dramatically with opening of the gate (Holmgren et al., 1997, 1998; Liu et al., 1997; del Camino and Yellen, 2001; Zhou et al., 2001). A comparison between the X-ray structures of two prokaryotic K^+ channels, the KcsA K^+ channel (Doyle et al., 1998), which is thought to be closed (Roux et al., 2000; Zhou et al., 2001; Jiang et al., 2002a), and the Ca^{2+}-activated MthK channel, which is open (Jiang et al., 2002a), supports the notion of an intracellular gate that is formed by the TM2 helix, a region that corresponds to S6 in K_v channels (Jiang et al., 2002b). In the prokaryotic channels, opening of the intracellular gate has been proposed to involve bending of the TM2 helices at a glycine residue that is conserved in K^+ channels (red highlighting in Fig. 1 C), greatly widening the intracellular entrance to the ion conduction pathway. In contrast, several studies in K_v channels point to a unique structure of the intracellular pore region and a significantly smaller movement during opening (del Camino et al., 2000; del Camino and Yellen, 2001; Swartz, 2004; Webster et al., 2004).

Mutational studies on the intracellular gate region of K_v channels show that amino acid substitutions most frequently shift the closed–open equilibrium in favor of the open state (Hackos et al., 2002; Yifrach and MacKinnon, 2002). This observation can be explained if the closed conformation of the channel is intrinsically

Address correspondence to Kenton J. Swartz, Molecular Physiology and Biophysics Section, National Institute of Neurological Disorders and Stroke, National Institutes of Health, Porter Neuroscience Research Center, 3B-215, 35 Convent Dr., MSC 3701, Bethesda, MD 20892-3701. Fax: (301) 435-5666; email: swartzk@ninds.nih.gov

Abbreviations used in this paper: TEA, tetraethylammonium; TM, transmembrane.

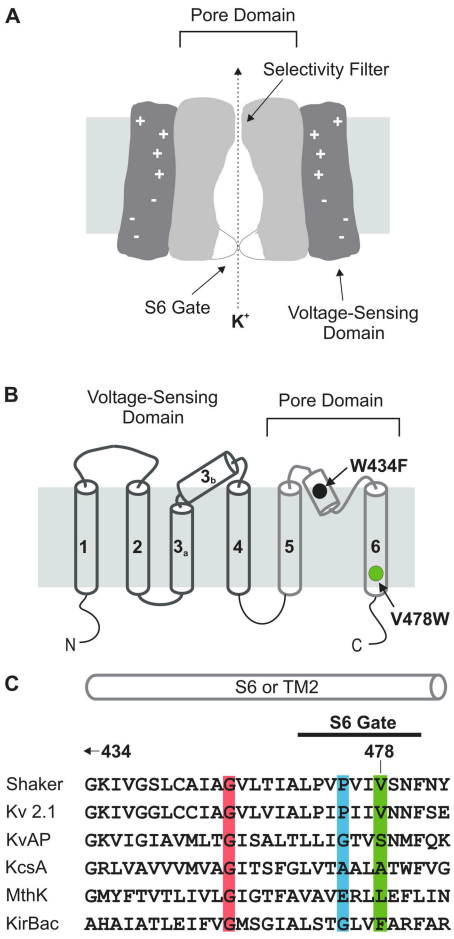

FIGURE 1. The intracellular gate region of K^+ channels. (A) Cartoon of a voltage-gated K^+ channel showing separate voltage-sensing and pore domains and the S6 activation gate toward the intracellular side of the pore. (B) Membrane folding diagram for a K_v channel showing six TM domains. S1–S4 comprise the voltage-sensing domains, while S5–S6 forms the pore domain. Black circle in pore region illustrates the position of W434 and green circle in activation gate region illustrates the position of V478. (C) Sequence alignment between K_v channels, KcsA, MthK, and KirBac. Red highlighting marks the conserved Gly residue that is proposed to serve as the gating hinge (Jiang et al., 2002a,b). Blue highlighting marks the position of P475 in Shaker, corresponding to P406 in K_v2.1, G229 in K_vAP, A108 in KcsA, E92 in MthK, and G143 in KirBac. Green highlighting marks positions equivalent to V478 in Shaker, where W substitutions result in nonconducting channels (Hackos et al., 2002).

more stable, and thus easier to perturb than the open conformation (Yifrach and MacKinnon, 2002). The KcsA and MthK structures support this notion because the intracellular gate region in the closed KcsA structure is significantly more compact, and exhibits less solvent exposure, than the structure for the open MthK channel. An extreme example of destabilization of the closed conformation of the gate is seen for hydrophilic substitutions at P475 in the Shaker K_v channel (blue highlighting in Fig. 1 C), giving rise to constitutive activation even when the voltage sensors are at rest (Sukhareva et al., 2003). Although mutations in the gate region most commonly destabilize the closed state, there are specific positions where mutations prevent ion conduction. For example, mutation of V478 to W (green shading in Fig. 1 C) results in a channel that traffics to the plasma membrane, but does not conduct ions even though the voltage sensors remain competent to translocate gating charge (Hackos et al., 2002). This residue is particularly interesting because it is located in a critical region within the intracellular S6 gate and may play a role in limiting the flow of ions in the closed state (del Camino and Yellen, 2001; Hackos et al., 2002; Webster et al., 2004). In this paper we explore three types of mechanisms that might underlie the inability of V478W to conduct ions, a phenotype that we operationally refer to as nonconducting. One possibility is that the mutant channel is predominantly found in an inactivated state, similar to what has been previously shown for the W434F, a nonconducting mutation in the external region of the pore of the channel. Since the V478W mutation results in a substantial increase in side chain volume ($\sim$60 Å^3 per subunit), an alternate possibility is that the intracellular gate can open, but that a large barrier to ion permeation has been introduced by the mutation. A third explanation is that the mutation dramatically perturbs the closed–open equilibrium in a manner that does not interfere with activation of the voltage sensors, but prevents significant opening of the activation gate. Our results are most consistent with the mechanism of nonconduction that involves a relative stabilization of the closed state of the channel.

MATERIALS AND METHODS

Molecular Biology and Channel Expression

All experiments were performed using the Shaker H4 K_v channel in either Bluescript, pGEM-HE (Liman et al., 1992), or pCS2 vectors (Turner and Weintraub, 1994) with a deletion of residues 6–46 to remove fast N-type inactivation (Hoshi et al., 1990). Point mutations were generated through sequential PCR, and all mutations were verified by DNA sequencing. Heterodimer and homodimer constructs were produced by concatenating Shaker cDNAs with a 30-bp linker encoding the NNNNNNAMVE sequence.

Plasmids were linearized with HindIII, NheI or Not I, and cRNAs were transcribed with T7 or SP6 polymerase. *Xenopus laevis* oocytes were removed surgically and incubated with agitation for 60–90 min in solution containing (in mM) 82.5 NaCl, 2.5 KCl, 1 $MgCl_2$, 5 HEPES, and 2 mg/ml collagenase, pH 7.6 with NaOH. Defolliculated oocytes were injected with cRNA and incubated at 17°C in a solution containing (in mM) 96 NaCl, 2 KCl, 1 $MgCl_2$, 1.8 $CaCl_2$, 5 HEPES, and 50 μg/ml gentamicin, pH 7.6 with NaOH for 1–6 d before electrophysiological recording or harvesting of channel protein. Western analysis of protein expression was done using a c-myc epitope–tagged construct of Shaker as previously described (Hackos et al., 2002).

Electrophysiological Recording

Macroscopic ionic and gating current were recorded from expressed channels using two-electrode voltage clamp recording

techniques between 1 and 6 d after cRNA injection. For the majority of experiments, oocytes were studied in a solution containing (in mM) 50 RbCl, 50 NaCl, 1 $MgCl_2$, 0.3 $CaCl_2$, and 5 HEPES, pH 7.6 with NaOH. For the experiments described in Figs. 4 and 5, 100 mM KCl was used in place of RbCl and NaCl. For internal tetraethylammonium (TEA) experiments (Fig. 6), an injection pipette was used to inject oocytes with 100 nl of a 200 mM TEA solution during electrophysiological recording. If we assume an oocyte volume of 500 nl, the final intracellular concentration of TEA would be ~40 mM. With the exception of the experiments in Fig. 11, leak and linear capacity currents were subtracted using a P/−4 procedure (Bezanilla and Armstrong, 1974). For the experiments in Fig. 11, leak and linear capacity currents were subtracted by blocking the Shaker channel with Agitoxin-2 (Garcia et al., 1994) and subtracting the toxin-insensitive currents. Agitoxin-2 was also used to isolate ionic currents for the V478W-Wt dimer (Fig. 4) and for all weakly conducting mutants (Fig. 8), in addition to P/−4 subtraction to isolate gating currents.

To qualitatively characterize the gating behavior of various mutant channels, tail current voltage–activation relations (G-V) were fit with single Boltzmann functions according to: $G/G_{max} = (1 + e^{-zF(V - V50)/RT})^{-1}$. For mutants at V478 that produce robustly conducting channels (V478A, Q, S) a maximal conductance could be defined (Fig. 9) and used to normalize the G–V relations. For mutants that give rise to weakly conducting channels (V478M, I, L, C, T, N, and H), a maximal conductance could not be defined. In these instances, G_{max} was obtained by fitting the Boltzmann equation to conductance measurements available between −50 and +100 mV (Fig. 8). The G–V relation for V478W–Wt heterodimers was arbitrarily normalized to the conductance measure following depolarization to +100 mV.

Gating charge versus voltage (Q–V) relations were obtained by integrating both ON and OFF components of gating current and then fitting single Boltzmann functions to the average Q versus V relations according to: $Q/Q_{max} = (1 + e^{-zF(V - V50)/RT})^{-1}$. Unitary currents were recorded in inside-out patches using a patch-clamp amplifier (Axopatch 200B). Data were filtered at 2 kHz (8-pole Bessel) and digitized at 20 kHz. Patch pipette resistance filled with the recording solution was 10–15 MΩ. The intracellular (bath) solution contained (in mM) 140 KCl, 4 EGTA, 1 $CaCl_2$, 2 $MgCl_2$, 5 HEPES, pH 7.6. The extracellular (pipette) solution contained (in mM) 140 KCl, 1 $CaCl_2$, 2 $MgCl_2$, 5 HEPES, pH 7.6. We routinely examined patches from uninjected oocytes on the same days that we studied the mutant channels of Shaker and observed channel activity like that shown in Figs. 12 and 13 only with Shaker cRNA–injected oocytes. We also confirmed the sensitivity of Shaker single channel activity to Agitoxin-2 by routinely comparing successive patches with and without the toxin in the patch pipette.

To estimate open probabilities (P_o) we used two approaches. For the wild-type channel, multiple Gaussian functions were fit to the all points histogram for a given voltage and the relative areas of these functions used to estimate P_o. For the V478W–Wt dimer we used half-amplitude threshold analysis (Colquhoun and Sigworth, 1995) to idealize single-channel recordings for kinetic analysis using pClamp 9 (Axon Instruments, Inc.).

RESULTS

The objective of the present study is to understand the mechanism by which the V478W mutation in the Shaker K_v channel gives rise to a nonconducting phenotype. For most of the experiments described here, the V478W mutant was expressed in *Xenopus* oocytes and studied using two-electrode voltage clamp recording techniques with 50 mM Rb^+ and 50 mM Na^+ as the primary cations in the extracellular solution, and endogenous K^+ (~100 mM) as the primary cation in the intracellular solution. Under these recording conditions there is no evidence of ionic current, even when the channel is expressed to levels of $>10^8$ channels per cell (see below). However, gating currents can be observed at these expression levels (Fig. 2 A), indicating that the mutant channel efficiently traffics to the plasma membrane and retains functional voltage sensors. If we integrate the gating currents for the example of V478W shown in Fig. 2 A, we obtain a value of 22 nC for Q_{max}, which corresponds to $\sim 1 \times 10^9$ channels given a charge per channel to be 13.6 (Aggarwal and MacKinnon, 1996). The lack of ionic currents (<50 nA) in this example is quite dramatic if one considers that the amplitude of ionic currents would be in the low mA range for the wild-type channel at this expression level. The gating currents recorded for V478W, as well as the charge (Q) versus voltage (V) relation obtained by integrating both the ON and OFF components of gating current

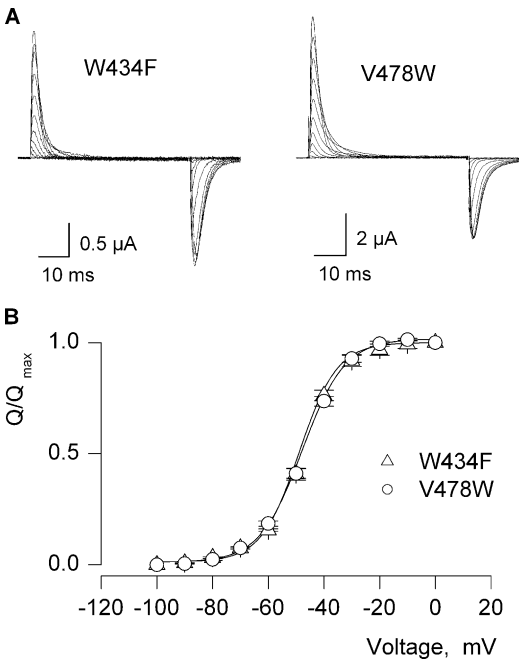

FIGURE 2. Gating currents and Q–V relations for two Shaker K_v channel mutants that display a nonconducting phenotype. (A) Families of gating currents for two mutant Shaker K^+ channels. For both families, holding voltage was −100 mV and depolarizations were to voltage between −100 mV and 0 mV with 10-mV increments. A P/−4 protocol was used to subtract leak and linear capacitive currents. (B) Normalized Q–V relations for W434F and V478W. Q was obtained by integrating both ON and OFF components of gating current, taking their average and normalized to Q_{max} measured at depolarized voltage. Data points are mean ± SEM. Smooth curves correspond to single Boltzmann functions with parameters as follows: W434F, V_{50} = −47.6 mV, z = 3.6; V478W, V_{50} = −47.3 mV, z = 3.2. See Table I for statistics.

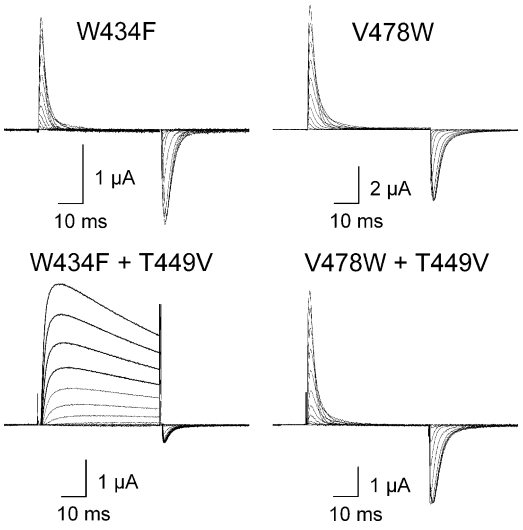

FIGURE 3. Effects of the T449V mutation on two nonconducting mutations in the Shaker K_v channel. Families of ionic and gating currents are shown for W434F and V478W, with and without the T449V mutation. For gating current families, holding voltage was −100 mV and depolarizations were from −100 to 0 mV, in 10-mV increments. For W434F+T449V, holding voltage was −100 mV, tail voltage was −100 mV, and depolarizations were from −100 to 40 mV, in 10-mV increments. A P/−4 protocol was used to subtract leak and linear capacitive currents.

(Fig. 2 B), are similar to those observed for the W434F (Perozo et al., 1993; Yang et al., 1997; Starkus et al., 1998), a well-studied mutation in the external pore of Shaker that also results in a nonconducting phenotype in the presence of permeant ions like K^+ or Rb^+.

Do the Nonconducting Phenotypes in W434F and V478W Have Similar Mechanisms?

Previous studies on the W434F mutation in the Shaker K_v channel suggest that this mutant is effectively nonconducting because it is predominantly found in a slow inactivated state (Yang et al., 1997). One observation supporting the proposed mechanism for W434F is that the T449V mutation within the selectivity filter has been shown to effectively eliminate the process of slow inactivation (Lopez-Barneo et al., 1993) and to rescue ion conduction in W434F (Yang et al., 2002). We first compared the effects of the T449V mutation on channels containing either the W434F or V478W mutations. Although the T449V mutation rescues ion conduction in W434F, consistent with previous findings, the mutation is without discernable effect on V478W (Fig. 3). The T449V/V478W double mutant displays gating currents that are similar to the V478W single mutant, but no evidence of ionic currents.

Another observation supporting the involvement of inactivation in the mechanism of nonconduction for W434F is that channels containing less than four mutant subunits are conducting, and the inactivation kinetics become progressively more rapid with increasing numbers of mutant subunits per channel (Yang et al., 1997). Before addressing whether a similar phenomenon exists for V478W, we examined whether V478W–Wt dimer supports ion conduction (Fig. 4 A). The ionic currents seen following expression of wild-type homodimers (Wt–Wt) and the gating currents for V478W homodimers (V478W–V478W) are indistinguishable from those seen for channels containing monomeric wild-type or V478W, respectively (Fig. 4 B). Expression of the V478W–Wt heterodimer gives rise to channels that conduct macroscopic ionic currents, similar to W434F, but only when expression reaches levels that are high enough to observe gating currents (Fig. 4 C). Ionic currents cannot be studied for the wild-type channel at these expression levels because they would be too large, in the mA range. The ionic currents in the V478–Wt dimer are sensitive to the pore blocking toxin Agitoxin-2 (Garcia et al., 1994), whereas the gating currents are toxin insensitive, allowing a clear distinction between the two types of currents (Fig. 4 C). The conductance (G) versus voltage (V) relation for the V478W–Wt heterodimer has a more shallow slope and appears to be shifted to more depolarized voltages compared with the wild-type channel (Fig. 4 D). The Q–V relation for the V478W–Wt dimer exhibits a small shift to more depolarized voltages, an effect that is probably attributable to Agitoxin-2 since we observed similar effects of the toxin on the monomeric V478W construct (unpublished data). Having observed voltage-activated ionic currents for the V478W–Wt heterodimer, we then examined the kinetics of slow inactivation using long depolarizing pulses to +40 mV (Fig. 5 A). The inactivation kinetics of the Wt–Wt, V478W–Wt, and Wt–V478W dimers are well described by single exponential functions where the time constant for the V478–Wt and Wt–V478W dimers are somewhat faster than the Wt–Wt dimer (Fig. 5 B). In contrast, the W434F–Wt and Wt–W434F dimers display double exponential kinetics with a fast component that is approximately an order of magnitude faster than inactivation observed for the Wt or V478W constructs (Fig. 5, A and B). Thus, although the V478W mutation has a small effect on inactivation kinetics, the magnitude of the effect is very different from what is observed for W434F. These results, together with the T449V rescue experiments, suggest that the mechanism underlying the nonconducting phenotype in V478W is distinct from that for W434F.

Does the Intracellular Activation Gate Move in Response to Depolarization?

Although channels containing four subunits carrying the W434F mutation do not conduct in the presence of permeant ions, intracellular blockers like tetraethylammonium (TEA) reveal that the intracellular gate still

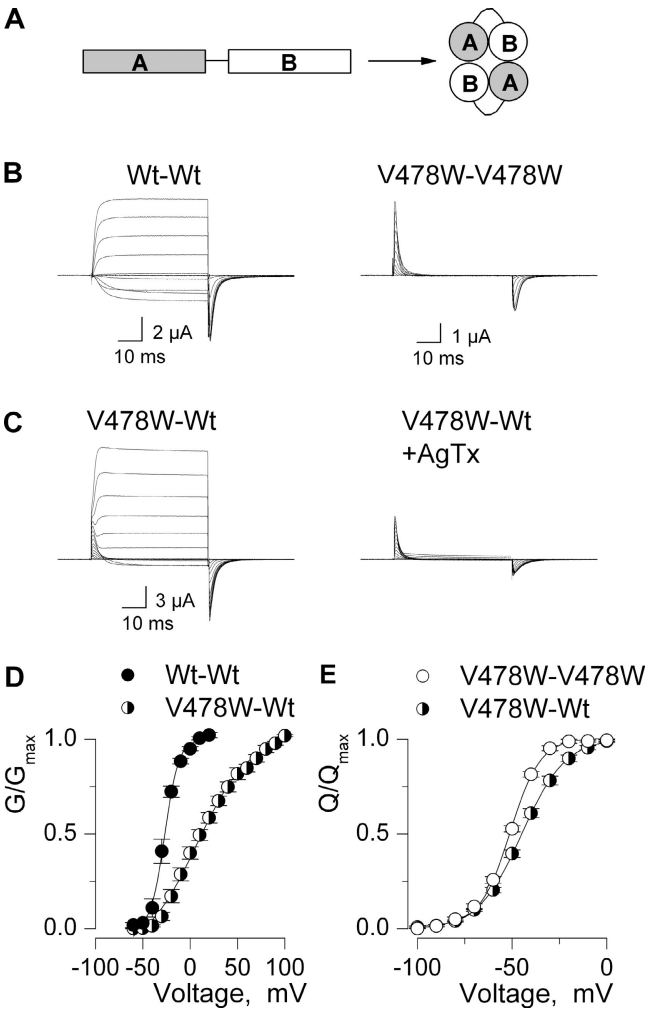

FIGURE 4. Ionic and gating currents for dimeric Shaker constructs. (A) Schematic diagram illustrating dimeric channel constructs. A and B protomers are concatenated using 10-residue linkers. (B) Families of ionic and gating currents for homodimers of Wt and V478W-containing subunits. For Wt–Wt, holding voltage is −100 mV, tail voltage was −60 mV, and depolarizations were from −60 to 40 mV, in 10-mV increments. For V478W–V478W, holding voltage was −100 mV and depolarizations were from −100 to 0 mV, in 10-mV increments. (C) Families of ionic and gating currents for the V478W–Wt heterodimer. Holding voltage was −100 mV and depolarizations were from −100 to 50 mV, in 10-mV increments, with or without 1 μM Agitoxin-2. A P/−4 protocol was used to subtract leak and linear capacitive currents. All constructs were recorded using an external solution containing 100 mM KCl. (D) G–V relations for Wt–Wt and V478W–Wt dimers. For Wt–Wt, normalized tail current amplitudes, measured at voltages indicated in B, are plotted versus the voltage of the preceding depolarization. For V478W–Wt, the ionic tail currents are significantly contaminated by OFF gating current and therefore conductance was calculated from the amplitude of steady-state current before repolarization, normalized to the value at +100 mV and plotted versus voltage. Agitoxin-2 was used to isolate ionic currents from endogenous currents. Data points are mean ± SEM. Smooth curves are single Boltzmann fits to the data with parameters as follows: Wt–Wt, V_{50} = −27 mV, z = 3.4; V478W–Wt, V_{50} = +7 mV, z = 1. (E) Normalized Q–V relations for V478W–V478W and V478W–Wt dimers. Q was obtained by integrating both ON and OFF components of gating current, taking their average and normalized to Q_{max} measured following strong depolarizations. Data points are mean ± SEM. Smooth curves are single Boltzmann fits to the data with parameters as follows: V478W–V478W, V_{50} = −51 mV, z = 3.2; V478W–Wt, V_{50} = −45 mV, z = 2.2. See Table I for statistics.

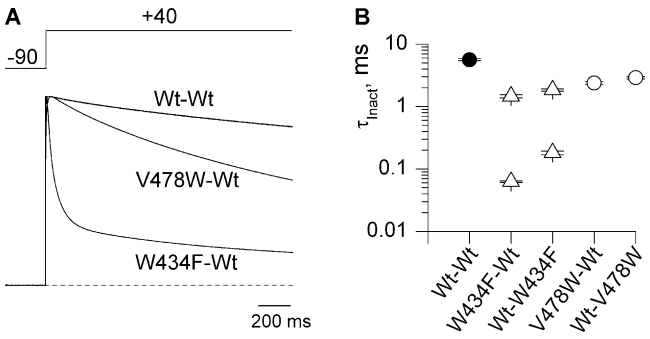

FIGURE 5. Inactivation kinetics for W434F and V478W dimers. (A) Current records for long test pulses to +40 mV. All constructs were recorded using an external solution containing 100 mM KCl. (B) Inactivation time constants for dimer constructs. Single exponential functions were fit to inactivating currents for Wt–Wt (n = 12), V478W–Wt (n = 6), and Wt–V478W (n = 14), while double exponential functions were fit to inactivating currents for W434F–Wt (n = 10) and Wt–W434F (n = 12) dimers. Data points are mean ± SEM.

opens and closes in response to changes in membrane voltage. In W434F, intracellular TEA slows the return of OFF gating charge because the blocker binds to the open conformation of the gate and prevents closure, an event that appears to be required for the voltage sensors to return to their resting conformations (Bezanilla et al., 1991; Perozo et al., 1993; Melishchuk and Armstrong, 2001). In effect, the kinetics of the decay of OFF gating current is a sensitive indicator of whether the intracellular gate moves between open and closed conformations even though the channel cannot conduct ions due to structural changes in the external vestibule. To address whether the intracellular activation gate moves in the V478W mutant, we examined the effects of intracellular TEA on the decay of the OFF gating current, performing parallel experiments with W434F as a control. To quantify the effects of TEA on gating current kinetics, we fit exponential functions to the decay of OFF component of gating current and plotted the resulting time constants (τ_{Qoff}) as a function of membrane voltage (Fig. 6). For the W434F channel, τ_{Qoff} is not affected by TEA when test pulses are given in the voltage range over which the gate remains closed (e.g., −80 mV to −60 mV). However, τ_{Qoff} displays a pronounced slowing in the presence of intracellular TEA when the membrane is depolarized to voltage between −50 mV and 0 mV, the range where the gate

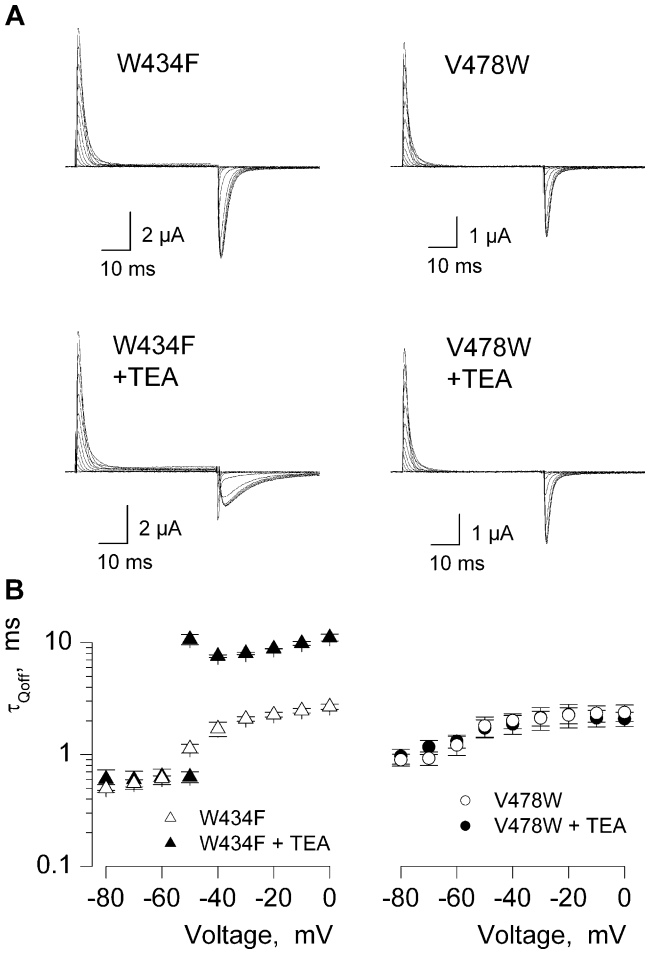

FIGURE 6. Effects of internal TEA on gating charge immobilization in two Shaker K_v channel mutants. (A) Families of gating currents for two Shaker mutants in the absence and presence of internal TEA. For all mutants, holding voltage was −100 mV and depolarizations were from −100 to 0 mV, in 10-mV increments. A P/−4 protocol was used to subtract leak and linear capacitive currents. (B) Plots of τ_{Qoff} against test voltage in the absence or presence of internal TEA. τ_{Qoff} was obtained by fitting single exponential functions to the time course of OFF gating currents. For W434F in the presence of TEA, following test depolarizations to −50 mV, a double exponential function was fit to the OFF gating current. Data points are mean ± SEM. $n = 3$ for V478W and $n = 4$ for W434F.

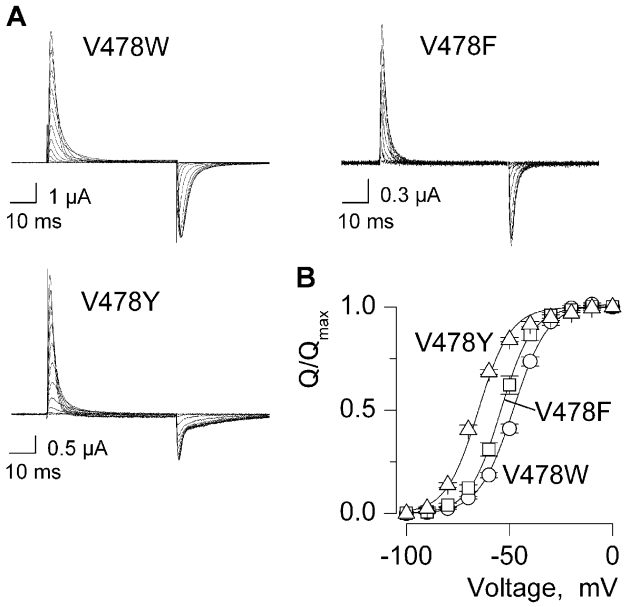

FIGURE 7. Gating currents and Q–V relations for Shaker K_v channels with aromatic substitutions at V478. (A) Families of gating currents for three mutant Shaker K_v channels. For all families, holding voltage was −100 mV and depolarizations were to voltage between −100 mV and 0 mV with 10-mV increments. A P/−4 protocol was used to subtract leak and linear capacitive currents. (B) Normalized Q–V relations. Q was obtained by integrating both ON and OFF components of gating current, taking their average and normalized to Q_{max} measured following strong depolarizations. Smooth curves are single Boltzmann fits to the data with parameters as follows: V478W, $V_{50} = -48$ mV, $z = 3.3$; V478F, $V_{50} = -54$ mV, $z = 3.3$; V478Y, $V_{50} = -66$ mV, $z = 2.9$. See Table I for statistics.

opens for the wild-type channel (Fig. 6). In the absence of TEA, there is a much smaller effect of membrane depolarization on the decay of OFF gating current, a phenomenon that may result from permeant ions occupying the cavity within the pore (Melishchuk and Armstrong, 2001). When identical experiments are performed with channels containing the V478W mutation, it is evident that τ_{Qoff} is unaffected by TEA (Fig. 6).

Although the effects of TEA on the W434F mutant nicely show that the activation gate moves with membrane depolarization, the lack of effect in the case of V478W has several possible interpretations. As described above, the effects of TEA on Q_{off} are thought to arise from the inability of the gate to close when the blocker is bound within the pore. One possibility is that the V478W mutation changes the internal pore region so that the activation gate can close with the blocker trapped inside the pore, as has been previously shown for the I470C mutation (Holmgren et al., 1997; Melishchuk and Armstrong, 2001). This seems unlikely because the V478W mutation quite dramatically increases side chain volume, opposite to what is observed at I470, where mutations that decrease side chain volume allow for trapping (Melishchuk and Armstrong, 2001). Another possibility is that the V478W mutation decreases the affinity of TEA so that the blocker can unbind faster, diminishing the effects of the blocker on the slowing of Q_{off}. However, the affinity of TEA for both the V478C (Holmgren, M., personal communication) and the P475Q/V478W double mutant (unpublished data) are unaltered, arguing against this possibility. In addition, it should be noted that neither of these two explanations for the lack of effect of TEA can explain why ion conduction is absent in the V478W mutant channel. The most straightforward implication for the

above results with TEA on V478W is that the channel is nonconducting either because the intracellular gate does not open or because a barrier in the open state prevents the movement of ions (and TEA). These experiments also provide an additional distinction for the mechanisms underlying the nonconducting phenotypes in W434F and V478W.

Phenotypes Resulting from Multiple Substitution at V478

If the V478W mutant creates a barrier to ion permeation by clogging the open gate, one might expect there to be a correlation between phenotype and side chain volume. To explore this possibility, we mutated V478 to all other residues and studied the functional properties of the resulting channels. When V478 was mutated to F and Y, the two other large aromatic residues, the resulting channels display a nonconducting phenotype that is similar to V478W (Fig. 7 A). The Q–V relations for V478F and V478Y are shifted to more negative voltage by 6 and 20 mV, respectively, when compared with V478W (Fig. 7 B; Table I). The slopes of the Q–V relations for all three aromatic substitutions are similar.

There are eight substitutions at V478 that result in channels that exhibit macroscopic ionic currents, but only at expression levels high enough to observe gating currents. This "weakly conducting" phenotype was observed for mutation of V478 to I, L, M, G, C, T, N, and H (Fig. 8; Table I). For all of these substitutions we verified that the ionic currents were sensitive to the pore blocker Agitoxin-2 and that the gating currents were toxin insensitive. The toxin sensitivity was particularly critical for mutants like V478M and V478G, where the ionic currents were quite small (Fig. 8, C and D). Interestingly, the G–V relations for all of these weakly conducting mutants display profound shifts to more positive voltages and large reductions in slope (Fig. 8 E; Table I), whereas the Q–V relation exhibits only modest changes (Fig. 8 F; Table I).

There were only three mutants that display large ionic currents at moderate expression levels. This "normal conducting" phenotype was observed for substitution of A, Q, and S for the wild-type V (Fig. 9 A). The G–V relations for V478A and V478Q exhibit small shifts to more negative voltages compared with the wild-type channel, whereas the V478S exhibits a small shift to more depolarized voltages (Fig. 9 B). The remaining five substitutions (R, K, E, D, and P) show no evidence of functional activity. We distinguished whether these channel are retained in the ER or whether they traffic to the plasma membrane but are nonfunctional by examining the extent of glycosylation (Santacruz-Toloza et al., 1994; Papazian et al., 1995; Schulteis et al., 1995). Western blots of SDS polyacrylamide gels show that the wild-type protein has two dominant forms, a core-glycosylated species (band ~70 kD) that is retained in the

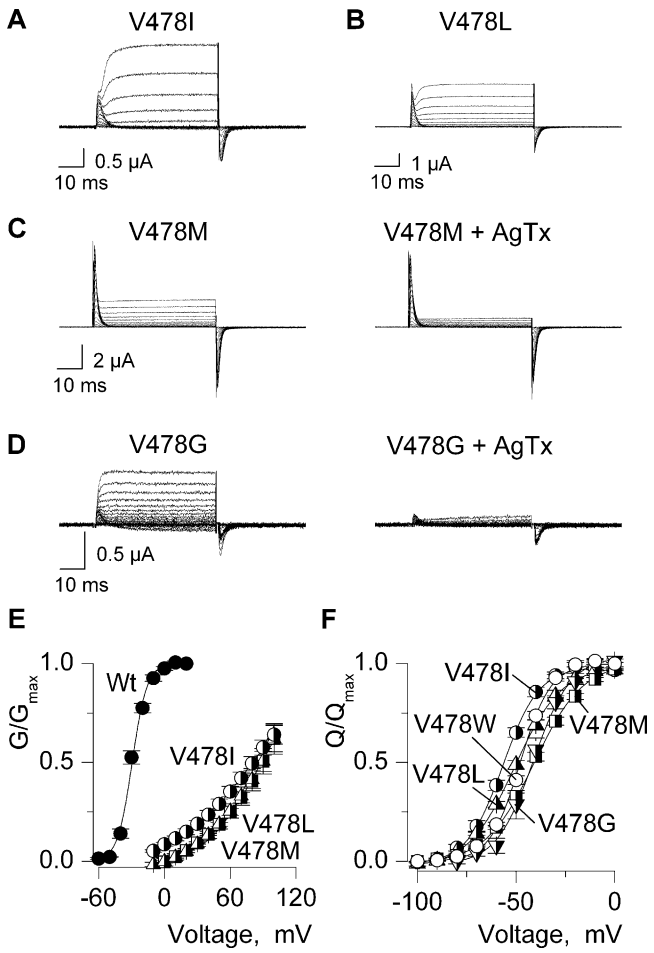

FIGURE 8. Gating properties of Shaker V478 mutants displaying weakly conducting phenotypes. (A) Family of ionic and gating currents for the V478I mutant. Holding voltage was −100 mV and depolarizations were from −90 to 30 mV, in 10-mV increments. (B) Family of ionic and gating current for the V478L mutant. Holding voltage was −100 mV and depolarizations were from −90 to 80 mV, in 10-mV increments. (C) Families of ionic and gating current for the V478M mutant in the absence or presence of 1 μM Agitoxin-2. Holding voltage was −100 mV and depolarizations were from −100 to 100 mV, in 10-mV increments. (D) Family of ionic and gating current for the V478G mutant in the absence or presence of 1 μM Agitoxin-2. Holding voltage was −100 mV and depolarizations were from −100 to 100 mV, in 10-mV increments. (E) G–V relations for three weakly conducting mutants. Conductance was calculated from the amplitude of steady-state current before repolarization, normalized to G_{max} estimated from Boltzmann fits and plotted versus voltage. Agitoxin-2 was used to isolate ionic currents from endogenous currents. Data points are mean ± SEM. Smooth curves are single Boltzmann fits to the data with parameters as follows: V478I, V_{50} = +88 mV, z = 1; V478L, V_{50} = +80 mV, z = 0.8; V478M, V_{50} = +89 mV, z = 1. (F) Normalized Q–V relations for three weakly conducting mutants. Q was obtained by integrating both ON and OFF components of gating current, taking their average and normalized to Q_{max} measured for strong depolarizations. Data points are mean ± SEM. Smooth curves are single Boltzmann fits to the data with parameters as follows: V478I, V_{50} = −56 mV, z = 2.8; V478L, V_{50} = −49 mV, z = 2.3; V478M, V_{50} = −41 mV, z = 2.1; V478G, V_{50} = −42 mV, z = 3.1; V478W, V_{50} = −48 mV, z = 3.3. In all instances a P/−4 protocol was used to subtract leak and linear capacitive currents. See Table I for statistics.

TABLE I

Gating Properties for Mutant Shaker K_v Channels

	(G–V)			(Q–V)		
Construct	V_{50}	z	*n*	V_{50}	z	*n*
Wt	−29.4 ± 0.9	3.9 ± 0.2	6	ND		
Nonconducting						
W434F				−47.3 ± 0.4	3.8 ± 0.1	9
V478W	ND			−47.8 ± 0.2	3.2 ± 0.1	5
V478F	ND			−53.7 ± 1.4	3.3 ± 0.1	7
V478Y	ND			−67.0 ± 0.4	3.2 ± 0.1	9
Conducting						
V478A	−39.5 ± 0.7	3.7 ± 0.2	7	ND		
V478Q	−36.9 ± 0.8	5.7 ± 0.4	6	ND		
V478S	−28.0 ± 0.4	2.9 ± 0.1	6	ND		
Weakly conducting						
V478M	+91.5 ± 6.0	1.0 ± 0.1	6	−41.8 ± 0.8	2.0 ± 0.1	6
V478I	+80.0 ± 5.0	0.8 ± 0.02	5	−56.2 ± 1.1	2.8 ± 0.6	7
V478L	+88.3 ± 7.1	1.1 ± 0.1	6	−50.0 ± 0.9	2.1 ± 0.1	6
V478G	ND			−41.9 ± 2.1	3.3 ± 0.5	4
V478C	+7.5 ± 4.5	1.1 ± 0.1	3	−37.5 ± 0.9	2.7 ± 0.1	3
V478T	+26.6 ± 5.8	0.9 ± 0.04	4	−30.9 ± 1.5	2.3 ± 0.1	3
V478N	+46.5 ± 4.6	1.0 ± 0.1	4	−46.1 ± 2.8	2.5 ± 0.5	3
V478H	+51.9 ± 2.3	0.9 ± 0.03	3	−52.7 ± 0.9	2.9 ± 0.1	3
Rescuing mutants						
P475D	−98.5 ± 2.3	3.3 ± 0.4	10	ND		
P475Q	−95.2 ± 1.0	2.6 ± 0.1	24	ND		
V478W+P475D	−16.7 ± 1.3	3.1 ± 0.1	6	ND		
V478W+P475Q	−44.5 ± 0.7	2.1 ± 0.1	5	ND		
Dimers						
Wt–Wt	−27.1 ± 1.6	3.6 ± 0.1	5	ND		
V478W–V478W	ND			−51.0 ± 0.6	3.2 ± 0.2	4
V478W–Wt	+10.8 ± 3.7	1.2 ± 0.1	5	−44.7 ± 1.2	2.2 ± 0.1	4

ER and a more heavily glycosylated mature form (band ~100 kD) that is located on the plasma membrane (Fig. 10 A). The N259Q/N263Q double mutant shows only single band at ~65 kD, marking the position of the unglycosylated protein. Although heavily glycosylated protein is observed for the V478W nonconducting mutant, all five electrophysiologically silent mutants display only the 70-kD core glycosylated form (Fig. 10 A), suggesting that they are largely retained within the ER.

Fig. 10 B summarizes the results for all substitutions at V478. The large volume aromatic substitutions are all nonconducting and the moderate volume hydrophobic substitutions are weakly conducting, perhaps indicating that volume and hydrophobicity are important determinants of phenotype for mutations at V478. However, the weakly conducting phenotype is also caused by substitution with G, a residue without a side chain, C, a hydrophobic residue that is smaller than the wild-type V, and both N and T, two rather polar residues. If we assume that the weakly conducting phenotype is a mild version of the nonconducting phenotype, then perhaps the most interesting finding is that the G–V relations for the former group display midpoints that are dramatically shifted to depolarized voltages with substantial reductions in slope. This result is consistent with the notion that substitutions at V478 cause a relative stabilization of the closed conformation of the gate.

Rescue of the V478W Nonconducting Mutant by Constitutively Active Mutants

Next we asked whether the nonconducting phenotype observed in V478W could be rescued by other secondary mutations. The possibility of rescue would seem less likely in the case of the simple clogging mechanism, but perhaps expected in the case of a stabilized closed gate. We tested two mutations, P475D and P475Q, which have previously been shown to constitutively activate the Shaker K_v channel by destabilizing the closed state of the channel (Sukhareva et al., 2003). Addition of either of these two mutations to the V478W mutation results in channels that exhibit robust voltage-activated ionic currents (Fig. 11 A). In the case of P475Q/V478W, the G–V relation is shifted toward more neg-

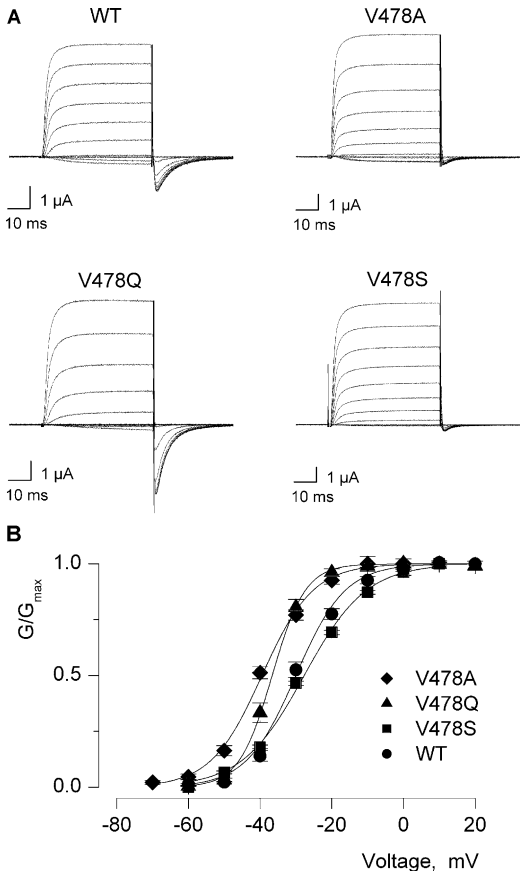

FIGURE 9. Gating properties of Shaker V478 mutants displaying a normal conducting phenotype. (A) Families of ionic currents for Wt Shaker and three normal conducting mutants. For Wt and V478A, holding voltage was −100 mV, tail voltage was −60 mV, and depolarizations were from −60 to 40 mV, in 10-mV increments. For V478Q, holding voltage was −100 mV, tail voltage was −100 mV, and depolarizations were from −90 to 20 mV, in 10-mV increments. For V478S, holding voltage was −100 mV, tail voltage was −50 mV, and depolarizations were from −50 to 50 mV, in 10-mV increments. A P/−4 protocol was used to subtract leak and linear capacitive currents. (B) G–V relations for Wt Shaker and three normal conducting mutants. In all cases, normalized tail current amplitudes, measured at voltages indicated in A, are plotted versus the voltage of the preceding depolarization. Data points are mean ± SEM. Smooth curves are single Boltzmann fits to the data with parameters as follows: Wt, V_{50} = −30 mV, z = 3.8; V478A, V_{50} = −40 mV, z = 3.6; V478Q, V_{50} = −37 mV, z = 5.5; V478S, V_{50} = −28 mV, z = 3. See Table I for statistics.

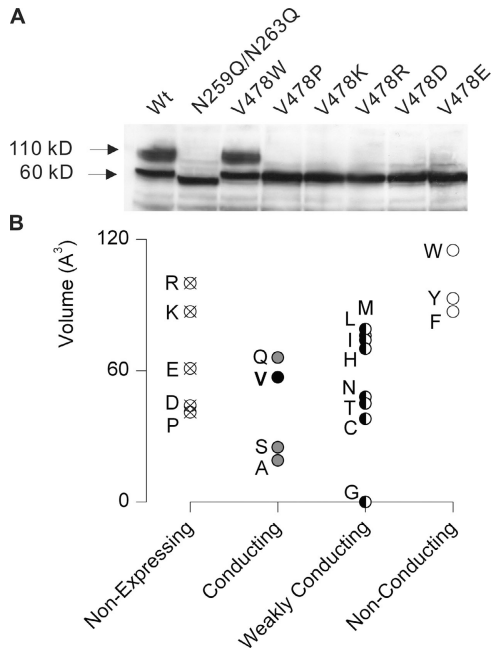

FIGURE 10. Nonexpressing mutants of the Shaker K_v channel and summary of phenotypes resulting from substitutions at V478. (A) Western blot from SDS polyacrylamide gel of c-myc–tagged Shaker protein obtained from oocyte membrane preparations. Each lane contains three oocyte equivalents of Shaker protein. Wt protein has two dominant forms, a core-glycosylated species (band ∼70 kD) and a more heavily glycosylated mature form (band at ∼100 kD). The N259Q/N263Q double mutant shows only a single band at ∼65 kD and marks the position of the unglycosylated protein. (B) Summary of phenotypes resulting from different substitutions at V478.

ative voltages compared with the wild-type channel, whereas in the case of P475D/V478W, the G–V relation is shifted toward more positive voltages (Fig. 11 B). The Agitoxin-2–sensitive macroscopic currents for either of these double mutants show no measurable standing current at negative voltages (Fig. 11, A and B), as if the P475 and V478 mutants largely compensate for one another. The rescue of ion conduction in V478W is most consistent with a nonconducting mechanism involving a shift of the closed to open equilibrium in favor of the closed state, an interpretation that fits nicely with previous evidence for constitutive activation by destabilizing the closed gated for hydrophilic substitutions at P475 (Sukhareva et al., 2003).

Is there a New Barrier to Ion Conduction in V478W?

To further examine whether the V478W mutation produces a new barrier to ion permeation we studied the unitary properties of two constructs that contain the V478W mutation but retain the ability to conduct ions. If the defect in the V478W mutation were solely a change in conductance we would expect that the conductance would be decreased by $>10^4$-fold compared with the wild-type channel. We first examined the V478W–Wt dimer (e.g., Fig. 4), a construct that produces channels with two mutations per channel, by recording single activity in symmetrical 140 mM KCl. The conductance of the highest conducting level for the wild-type channel is 24 pS under these recording conditions (Fig. 12, A and B). Channel activity similar to that shown in Fig. 12 A was observed in six patches for the dimer, with the channel exhibiting rather brief openings even at depolarized voltages. Although the all points histograms (not depicted) revealed poorly de-

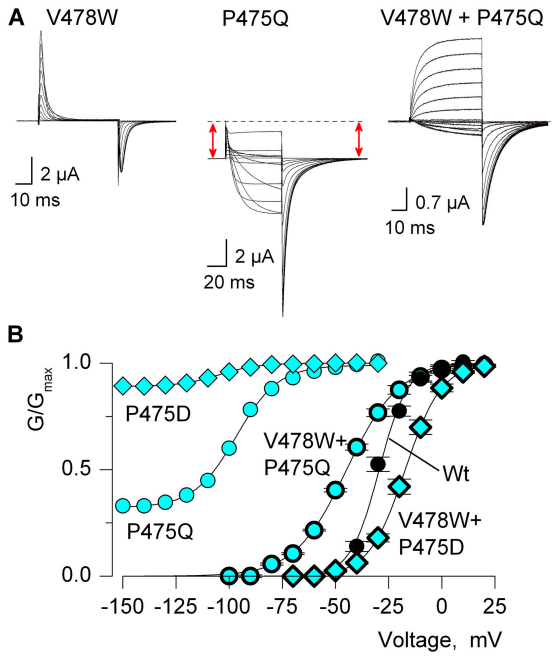

FIGURE 11. Rescue of ion conduction in V478W by secondary mutations at P475. (A) Families of gating and ionic current for V478W, P475Q, and the double mutant. For V478W, holding voltage was −100 mV, depolarizations were from −100 to 0 mV (10-mV increments) and a P/−4 protocol was used to subtract leak and linear capacitive currents. For P475Q, holding and tail voltages were −150 mV and depolarizations were from −150 to 30 mV, in 10-mV increments. For V478W/P475Q, holding and tail voltages were −100 mV and depolarizations were from −90 to 40 mV, in 10-mV increments. For both P475Q and V478W/P475Q, leak and linear capacitive currents were identified and subtracted by blocking the Shaker channel with Agitoxin-2. (B) G–V relations for Wt, two P475 mutants displaying constitutive activity and two double mutants displaying normal voltage-dependent gating. Normalized tail current amplitudes are plotted versus the voltage of the preceding depolarization. For P475D, the external solution contained 50 mM KCl, whereas for all other constructs the external solution contained 50 mM RbCl. Data points are mean ± SEM. Smooth curves are single Boltzmann fits to the data with parameters as follow: Wt, V_{50} = −30 mV, z = 3.8; P475Q, V_{50} = −97 mV, z = 2.6; P475D, V_{50} = −105 mV, z = 2.8; V478W/P475Q, V_{50} = −45 mV, z = 2.1; V478W/P475D, V_{50} = −17 mV, z = 3. See Table I for statistics.

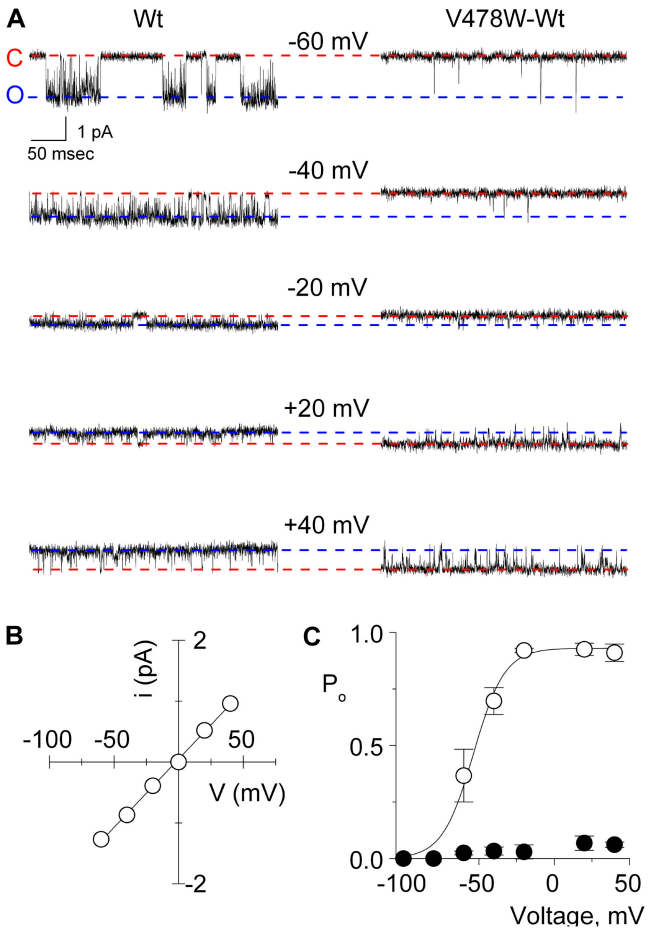

FIGURE 12. Single channel properties of Wt Shaker and the V478W–Wt dimer channel recorded in symmetrical K^+. (A) Representative current traces recorded from Wt Shaker (left) and V478W–Wt dimer (right) in symmetrical 140 mM KCl. The single channel patch was held at −100 mV and stepped from −100 mV to +40 mV with 20-mV increments for 400 ms and returned back to −100 mV. The traces represent segments of current records during the test pulse where single channel current events are observed. Filter frequency was 2 kHz. Horizontal dashed red and blue lines correspond to the closed and open current levels, respectively. (B) I–V relationship for the open state of the Wt Shaker channel. Linear regression of the shown data yields a conductance of 24 pS. (C) Open probability for the highest conducting state as a function of voltage for Wt (open circles) and for V478W–Wt dimer (filled circles). Smooth curve for Wt is a fit of a single Boltzmann function to the data with V_{50} = −54 mV and z = 2.5. Each data point represents the mean ± SEM (n = 5–6).

fined conductance levels, it is evident from the examples shown in Fig. 12 that there are openings to conductance levels that are indistinguishable from the wild-type channel. This observation, together with the low probability of opening (Fig. 12 C), is most consistent with a greatly perturbed closed–open equilibrium rather than a large change in unitary conductance.

We also studied the P475Q/V478W double mutant in which there are four V478W mutant subunits per channel. We recorded activity like that illustrated in Fig. 13 in eight patches under the same conditions described for the dimer. Although the all points histograms for both P475Q and the double mutant are complex (not depicted), it appears that the unitary conductance of the double mutant is no more than 50% smaller than the P475Q mutant. We conclude that the V478W mutation does not create a large barrier to ion conduction.

DISCUSSION

The objective of this study was to constrain the mechanism underlying the nonconducting phenotype observed for the V478W mutation in the Shaker K_v chan-

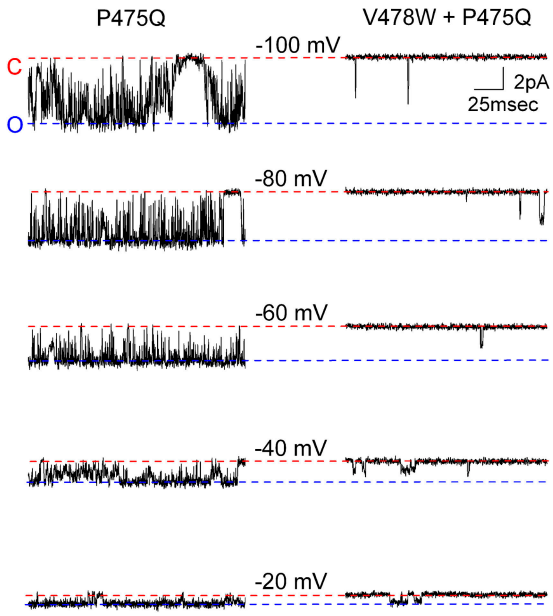

FIGURE 13. Single channel properties of the Shaker P475Q and V478W+P475Q mutant channel. (A) Representative current traces recorded for P475Q (left) and V478W+P475Q (right) in symmetrical 140 mM KCl. The single channel patch was held at −100 mV and stepped from −100 mV to 0 mV with 20-mV increments for 400 ms and returned back to −100 mV. The traces represent segments from current records where single channel current events were observed. Filter frequency was 2 kHz. Horizontal dashed red and blue lines correspond to the closed and open current levels for single mutant, respectively.

nel. Three observations suggest that the mechanism is distinct from that giving rise to nonconduction in W434F. First, the T449V mutation essentially disrupts slow inactivation in Shaker and rescues ion conduction in the W434F (Lopez-Barneo et al., 1993; Yang et al., 2002), but does not rescue ion conduction in V478W (Fig. 3). Second, although there is a correlation between the number of mutant subunits and the kinetics of inactivation for W434F (Yang et al., 1997), the results are quite different for V478W. Heterodimers containing V478W and wild-type subunits form channels that are competent to conduct ions (Fig. 4), but display inactivation kinetics that are rather similar to the wild-type channel (Fig. 5). A final distinction between W434F and V478W emerges from experiments probing the conformation of the internal pore with blockers of the open state. Although TEA slows the kinetics of Q_{off} for the W434F channel, suggesting that the intracellular activation gate remains competent to open following activation of the voltage sensors, the blocker has no effect on the V478W channel (Figs. 6). Thus it seems likely that the mechanisms underlying the absence of conduction in W434F and V478W are distinct.

One explanation for the lack of effect of TEA in the V478W channel is that the S6 activation gate does not open because the mutation causes a relative stabilization of the closed conformation. Alternately, perhaps the gate opens and closes but the V478W mutation has introduced a large barrier to ion permeation or to blocker entry into the pore. To explore this latter possibility we first attempted to rescue ion conduction by the addition of secondary mutations (P475Q,D) previously shown to destabilize the closed conformation (Sukhareva et al., 2003). Remarkably, ion conduction was restored in both the V478W/P475Q and V478W/P475D double mutants, in addition to relatively wild-type–like gating behavior (Fig. 11). If we assume that the aperture of the open state is not dramatically altered by the P475Q,D mutations, this result suggests that both types of mutations have opposite effects on the relative stability of the closed state. The restoration of ion conduction and voltage-dependent gating also suggests that neither of these mutants grossly disrupts the structure of the intracellular entrance to the pore. To further examine whether the V478W introduces a barrier to ion permeation we studied the unitary properties of two conducting constructs that contain the V478W mutation. If the primary defect in the V478W mutation is a decrease in ion throughput rate we would expect to see a $>10^4$-fold decrease in conductance. In the case of the V478W–Wt dimer, the openings of the channel are brief and rare, but at least some events appear to be to a conductance level similar to the wild-type channel (Fig. 12). Although the open probability is also low for the V478W/P475Q double mutant, the conductance of the highest conductance level is no more than 50% smaller when compared with the P475Q single mutant (Fig. 13). These single channel recordings with channels containing two (dimers) and four (double mutant) V478W mutations emphasize that the primary defect in the V478W mutation is in the gating of the channel and that the conduction properties, although perturbed, cannot explain the nonconducting phenotype. We conclude that the V478W mutation causes the nonconducting phenotype by shifting the closed to open equilibrium toward the closed state.

Comparison with the Effects of Other Mutations and 4-Aminopyridine

Scheme I is a simplified conceptual model of two types of conformational changes that occur during activation of K_v channels. In this scheme, each of the four voltage sensors undergoes a voltage-dependent conformational change independently followed by a voltage-dependent concerted opening transition (Hoshi et al., 1994; Zagotta et al., 1994a,b; Schoppa and Sigworth, 1998a,b,c; Smith-Maxwell et al., 1998a,b; Ledwell and Aldrich, 1999; Horn et al., 2000; Mannuzzu and Isacoff, 2000).

$$(C_1 \xrightarrow{K_v} C_2)^4 \xrightarrow{L} O \qquad \text{(SCHEME 1)}$$

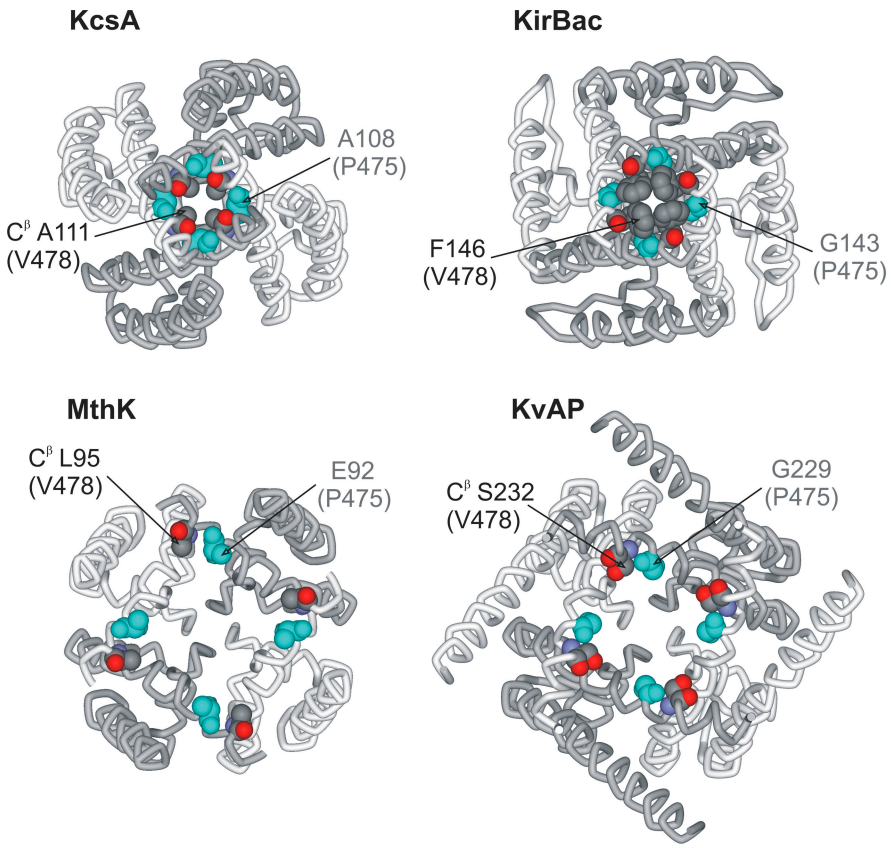

FIGURE 14. Pore structures of four K^+ channels viewed from an intracellular vantage point. In all instances, residues at the position equivalent to V478 are shown as CPK with carbon colored gray, oxygen colored red, and nitrogen colored blue. See Fig. 1 for sequence alignment. Residues at the equivalent position to P475 are shown in CPK with all atoms colored light blue. PDB accession code for KcsA is 1J95. PDB coordinates for KirBac provided by D.A. Doyle (University of Oxford, Oxford, UK). PDB accession code for MthK is 1LNQ. For MthK, E92 was modeled as an Ala. PDB accession code for K_vAP is 1ORQ. Structures were generated using DS Viewer Pro (Accelrys).

The present results are consistent with the idea that the V478W mutation causes a relative stabilization of the closed states by primarily altering L. Previous studies of the V2 and ILT mutants of Shaker suggest that these mutations alter the final concerted opening transition (Hoshi et al., 1994; Zagotta et al., 1994a,b; Schoppa and Sigworth, 1998a,b,c; Smith-Maxwell et al., 1998a,b; Ledwell and Aldrich, 1999; Horn et al., 2000; Mannuzzu and Isacoff, 2000). In the case of V2 and ILT, the P_o–V relation is shifted to more depolarized voltages and exhibits a reduced slope, similar to what is seen for many mutations at V478 (Fig. 8). The V2 and ILT mutants do not dramatically alter the maximal value of P_o, an observation that is consistent with the concerted opening transition having significant voltage dependence. We cannot measure opening for the V478W tetramer because it is nonconducting, and for the weakly conducting mutants, the macroscopic conductance continues to increase even at voltages as positive as +100 mV, so we cannot determine the maximal P_o for these mutants. However, the apparent maximal P_o observed for the V478W–Wt dimer and for the V478W/P475Q double mutant are <0.1, which is significantly less than the value of ~0.8 observed for the wild-type channel. Thus, our results leave open the possibility that the V478W mutation, unlike V2 and ILT, decreases the maximal P_o. The addition of a final opening transition that is voltage independent could account for an effect of V478W on maximal P_o. It is not surprising that there will be differences in the details of how these various mutations stabilize the closed state considering that the ILT mutations are located within the voltage-sensing S4 and the V2 mutant is in the linker between S4 and S5, whereas V478W is located within the gate itself.

The present interpretation for the effects of V478W on stabilizing the closed conformation of the gate is also reminiscent of the effects of 4-aminopyridine, a small organic compound that inhibits several types of K_v channels, including Shaker (Armstrong and Loboda, 2001; Loboda and Armstrong, 2001). Loboda and Armstrong proposed that when 4-aminopyridine binds to the cavity above the gate region, the blocker greatly stabilizes the closed conformation of the gate, effectively abolishing the final opening step once bound. Although the concerted transition governed by L is normally biased in favor of the open state, supporting maximal open probabilities around 0.8, 4-aminopyridine dramatically alters this equilibrium to favor the closed states without dramatically affecting voltage sensor activation. Although the observations supporting this mechanism were obtained from gating current measurements, the effects of 4-aminopyridine are rather subtle, causing only a 12-mV shift in the Q–V

curve, a 5% inhibition of maximal charge movement at depolarized voltages and a modest speeding of Q_{off} kinetics (Loboda et al., 2001). The present results with V478W were obtained using a significantly slower voltage clamp technique (1–2 ms settling times), and we have not determined the effects of the V478W mutation on the total charge per channel, so most likely the relatively unaltered gating currents observed here are not inconsistent with the small changes reported for 4-aminopyridine.

Structural Mechanism of Closed State Stabilization

Can a relative stabilization of the closed state by V478W be understood in the context of the structure of the gate region in potassium channels? So far there are four potassium channel structures that have been solved by X-ray diffraction. The KcsA (Doyle et al., 1998) and KirBac (Kuo et al., 2003) channels are thought to be closed, and the MthK (Jiang et al., 2002a,b) channel is open. Using KcsA and MthK as guides, the K_vAP structure appears to be more open than closed (Jiang et al., 2003), but distortions of the voltage sensor in this structure complicate assignment of gate conformation. The residues in these prokaryotic channels that align with V478 in Shaker (Fig. 1) are oriented such that the side chain projects toward the central axis of the pore (Figs. 1 and 14). In KcsA and KirBac, the two closed channels, the equivalent residues to V478 (gray CPK filling) are positioned at the narrowest part of the pore where hydrophobic interactions at the central axis would be predicted to stabilize the closed structure. Armstrong has discussed the concept of "hydrophobic seals" in KcsA, a feature that may serve to prevent ion flow in the closed state (Armstrong, 2003). In KcsA, there are three hydrophobic seals, at positions 107, 111, and 115, with A111 corresponding to V478 in Shaker. KirBac gives a particularly tantalizing glimpse into what aromatic substitutions might look like because the residue at this position in the wild-type channel is a phenylalanine (Fig. 14). In MthK and K_vAP, the residues equivalent to V478 are pore lining, but do not interact with the equivalent residue on other subunits because of the enlarged entrances to the pore in these more open channels. From these structures alone one might reasonably predict that large hydrophobic residues at positions equivalent to V478 would dramatically stabilize the closed conformation by strengthening the second hydrophobic seal of Armstrong.

It should be noted that many K_v channels, including the Shaker channel, contain a PVP motif just above V478 (Fig. 1). This unique feature of K_v channels has been proposed to bend the S6 helix in a manner that retains the orientation of the V478 side chain at the central axis, but removes the third hydrophobic seal of Armstrong (del Camino et al., 2000; del Camino and Yellen, 2001; Swartz, 2004; Webster et al., 2004). In this modified picture of the activation gate of Shaker, V478 is proposed to be the occluding residue in the closed state, a result that fits nicely with the nonconducting phenotype and the underlying mechanism studied here.

We thank Miguel Holmgren, Shai Silberberg, and members of the Swartz laboratory for helpful discussions and critique of the manuscript.

Olaf S. Andersen served as editor.

Submitted: 13 May 2004
Accepted: 13 August 2004

REFERENCES

Aggarwal, S.K., and R. MacKinnon. 1996. Contribution of the S4 segment to gating charge in the Shaker K^+ channel. *Neuron.* 16: 1169–1177.

Armstrong, C.M. 1969. Inactivation of the potassium conductance and related phenomena caused by quaternary ammonium ion injection in squid axons. *J. Gen. Physiol.* 54:553–575.

Armstrong, C.M. 1971. Interaction of tetraethylammonium ion derivatives with the potassium channels of giant axons. *J. Gen. Physiol.* 58:413–437.

Armstrong, C.M. 2003. Voltage-gated K channels. *Sci STKE.* 2003: re10.

Armstrong, C.M., and B. Hille. 1972. The inner quaternary ammonium ion receptor in potassium channels of the node of Ranvier. *J. Gen. Physiol.* 59:388–400.

Armstrong, C.M., and A. Loboda. 2001. A model for 4-aminopyridine action on K^+ channels: similarities to tetraethylammonium ion action. *Biophys. J.* 81:895–904.

Bezanilla, F., and C.M. Armstrong. 1974. Gating currents of the sodium channels: three ways to block them. *Science.* 183:753–754.

Bezanilla, F., E. Perozo, D.M. Papazian, and E. Stefani. 1991. Molecular basis of gating charge immobilization in Shaker potassium channels. *Science.* 254:679–683.

Colquhoun, D., and F.J. Sigworth. 1995. Fitting and statistical analysis of single-channel records. *In* Single-Channel Recording. B. Sakmann and E. Neher, editors. Plenum Publications, Inc., New York. 483–588.

del Camino, D., and G. Yellen. 2001. Tight steric closure at the intracellular activation gate of a voltage-gated K^+ channel. *Neuron.* 32:649–656.

del Camino, D., M. Holmgren, Y. Liu, and G. Yellen. 2000. Blocker protection in the pore of a voltage-gated K^+ channel and its structural implications. *Nature.* 403:321–325.

Doyle, D.A., J.M. Cabral, R.A. Pfuetzner, A. Kuo, J.M. Gulbis, S.L. Cohen, B.T. Chait, and R. MacKinnon. 1998. The structure of the potassium channel: molecular basis of K^+ conduction and selectivity. *Science.* 280:69–77.

Garcia, M.L., M. Garcia-Calvo, P. Hidalgo, A. Lee, and R. MacKinnon. 1994. Purification and characterization of three inhibitors of voltage-dependent K^+ channels from *Leiurus quinquestriatus* var. hebraeus venom. *Biochemistry.* 33:6834–6839.

Hackos, D.H., T.H. Chang, and K.J. Swartz. 2002. Scanning the intracellular s6 activation gate in the shaker K^+ channel. *J. Gen. Physiol.* 119:521–532.

Hille, B. 2001. Ion Channels of Excitable Membranes. 3rd ed. Sinauer, Sunderland, MA. 814 pp.

Holmgren, M., P.L. Smith, and G. Yellen. 1997. Trapping of organic

blockers by closing of voltage-dependent K^+ channels: evidence for a trap door mechanism of activation gating. *J. Gen. Physiol.* 109:527–535.

Holmgren, M., K.S. Shin, and G. Yellen. 1998. The activation gate of a voltage-gated K^+ channel can be trapped in the open state by an intersubunit metal bridge. *Neuron.* 21:617–621.

Horn, R., S. Ding, and H.J. Gruber. 2000. Immobilizing the moving parts of voltage-gated ion channels. *J. Gen. Physiol.* 116:461–476.

Hoshi, T., W.N. Zagotta, and R.W. Aldrich. 1990. Biophysical and molecular mechanisms of Shaker potassium channel inactivation. *Science.* 250:533–538.

Hoshi, T., W.N. Zagotta, and R.W. Aldrich. 1994. Shaker potassium channel gating. I: transitions near the open state. *J. Gen. Physiol.* 103:249–278.

Jiang, Y., A. Lee, J. Chen, M. Cadene, B.T. Chait, and R. MacKinnon. 2002a. Crystal structure and mechanism of a calcium-gated potassium channel. *Nature.* 417:515–522.

Jiang, Y., A. Lee, J. Chen, M. Cadene, B.T. Chait, and R. MacKinnon. 2002b. The open pore conformation of potassium channels. *Nature.* 417:523–526.

Jiang, Y., A. Lee, J. Chen, V. Ruta, M. Cadene, B.T. Chait, and R. MacKinnon. 2003. X-ray structure of a voltage-dependent K^+ channel. *Nature.* 423:33–41.

Kuo, A., J.M. Gulbis, J.F. Antcliff, T. Rahman, E.D. Lowe, J. Zimmer, J. Cuthbertson, F.M. Ashcroft, T. Ezaki, and D.A. Doyle. 2003. Crystal structure of the potassium channel KirBac1.1 in the closed state. *Science.* 300:1922–1926.

Ledwell, J.L., and R.W. Aldrich. 1999. Mutations in the S4 region isolate the final voltage-dependent cooperative step in potassium channel activation. *J. Gen. Physiol.* 113:389–414.

Liman, E.R., J. Tytgat, and P. Hess. 1992. Subunit stoichiometry of a mammalian K^+ channel determined by construction of multimeric cDNAs. *Neuron.* 9:861–871.

Liu, Y., M. Holmgren, M.E. Jurman, and G. Yellen. 1997. Gated access to the pore of a voltage-dependent K^+ channel. *Neuron.* 19: 175–184.

Loboda, A., and C.M. Armstrong. 2001. Resolving the gating charge movement associated with late transitions in K^+ channel activation. *Biophys. J.* 81:905–916.

Loboda, A., A. Melishchuk, and C. Armstrong. 2001. Dilated and defunct K^+ channels in the absence of K^+. *Biophys. J.* 80:2704–2714.

Lopez-Barneo, J., T. Hoshi, S.H. Heinemann, and R.W. Aldrich. 1993. Effects of external cations and mutations in the pore region on C-type inactivation of Shaker potassium channels. *Receptors Channels.* 1:61–71.

Mannuzzu, L.M., and E.Y. Isacoff. 2000. Independence and cooperativity in rearrangements of a potassium channel voltage sensor revealed by single subunit fluorescence. *J. Gen. Physiol.* 115:257–268.

Melishchuk, A., and C.M. Armstrong. 2001. Mechanism underlying slow kinetics of the OFF gating current in Shaker potassium channel. *Biophys. J.* 80:2167–2175.

Papazian, D.M., X.M. Shao, S.A. Seoh, A.F. Mock, Y. Huang, and D.H. Wainstock. 1995. Electrostatic interactions of S4 voltage sensor in Shaker K^+ channel. *Neuron.* 14:1293–1301.

Perozo, E., R. MacKinnon, F. Bezanilla, and E. Stefani. 1993. Gating currents from a nonconducting mutant reveal open-closed conformations in Shaker K^+ channels. *Neuron.* 11:353–358.

Roux, B., S. Berneche, and W. Im. 2000. Ion channels, permeation, and electrostatics: insight into the function of KcsA. *Biochemistry.* 39:13295–13306.

Santacruz-Toloza, L., E. Perozo, and D.M. Papazian. 1994. Purification and reconstitution of functional Shaker K^+ channels assayed with a light-driven voltage-control system. *Biochemistry.* 33:1295–1299.

Schoppa, N.E., and F.J. Sigworth. 1998a. Activation of shaker potassium channels. I. Characterization of voltage-dependent transitions. *J. Gen. Physiol.* 111:271–294.

Schoppa, N.E., and F.J. Sigworth. 1998b. Activation of Shaker potassium channels. II. Kinetics of the V2 mutant channel. *J. Gen. Physiol.* 111:295–311.

Schoppa, N.E., and F.J. Sigworth. 1998c. Activation of Shaker potassium channels. III. An activation gating model for wild-type and V2 mutant channels. *J. Gen. Physiol.* 111:313–342.

Schulteis, C.T., S.A. John, Y. Huang, C.Y. Tang, and D.M. Papazian. 1995. Conserved cysteine residues in the shaker K^+ channel are not linked by a disulfide bond. *Biochemistry.* 34:1725–1733.

Smith-Maxwell, C.J., J.L. Ledwell, and R.W. Aldrich. 1998a. Role of the S4 in cooperativity of voltage-dependent potassium channel activation. *J. Gen. Physiol.* 111:399–420.

Smith-Maxwell, C.J., J.L. Ledwell, and R.W. Aldrich. 1998b. Uncharged S4 residues and cooperativity in voltage-dependent potassium channel activation. *J. Gen. Physiol.* 111:421–439.

Starkus, J.G., L. Kuschel, M.D. Rayner, and S.H. Heinemann. 1998. Macroscopic Na^+ currents in the "Nonconducting" Shaker potassium channel mutant W434F. *J. Gen. Physiol.* 112:85–93.

Sukhareva, M., D.H. Hackos, and K.J. Swartz. 2003. Constitutive activation of the Shaker K_v channel. *J. Gen. Physiol.* 122:541–556.

Swartz, K.J. 2004. Opening the gate in potassium channels. *Nat. Struct. Mol. Biol.* 11:499–501.

Turner, D.L., and H. Weintraub. 1994. Expression of achaete-scute homolog 3 in *Xenopus* embryos converts ectodermal cells to a neural fate. *Genes Dev.* 8:1434–1447.

Webster, S.M., D. Del Camino, J.P. Dekker, and G. Yellen. 2004. Intracellular gate opening in Shaker K^+ channels defined by high-affinity metal bridges. *Nature.* 428:864–868.

Yang, Y., Y. Yan, and F.J. Sigworth. 1997. How does the W434F mutation block current in Shaker potassium channels? *J. Gen. Physiol.* 109:779–789.

Yang, Y., Y. Yan, and F.J. Sigworth. 2002. The Shaker mutation T449V rescues ionic currents of W434F K^+ channels. *Biophys. J.* 82:234e.

Yellen, G. 1998. The moving parts of voltage-gated ion channels. *Q. Rev. Biophys.* 31:239–295.

Yifrach, O., and R. MacKinnon. 2002. Energetics of pore opening in a voltage-gated K^+ channel. *Cell.* 111:231–239.

Zagotta, W.N., T. Hoshi, and R.W. Aldrich. 1994a. Shaker potassium channel gating. III: Evaluation of kinetic models for activation. *J. Gen. Physiol.* 103:321–362.

Zagotta, W.N., T. Hoshi, J. Dittman, and R.W. Aldrich. 1994b. Shaker potassium channel gating. II: Transitions in the activation pathway. *J. Gen. Physiol.* 103:279–319.

Zhou, M., J.H. Morais-Cabral, S. Mann, and R. MacKinnon. 2001. Potassium channel receptor site for the inactivation gate and quaternary amine inhibitors. *Nature.* 411:657–661.